

Supplemental material

Collins et al., <https://doi.org/10.1083/jcb.201804163>

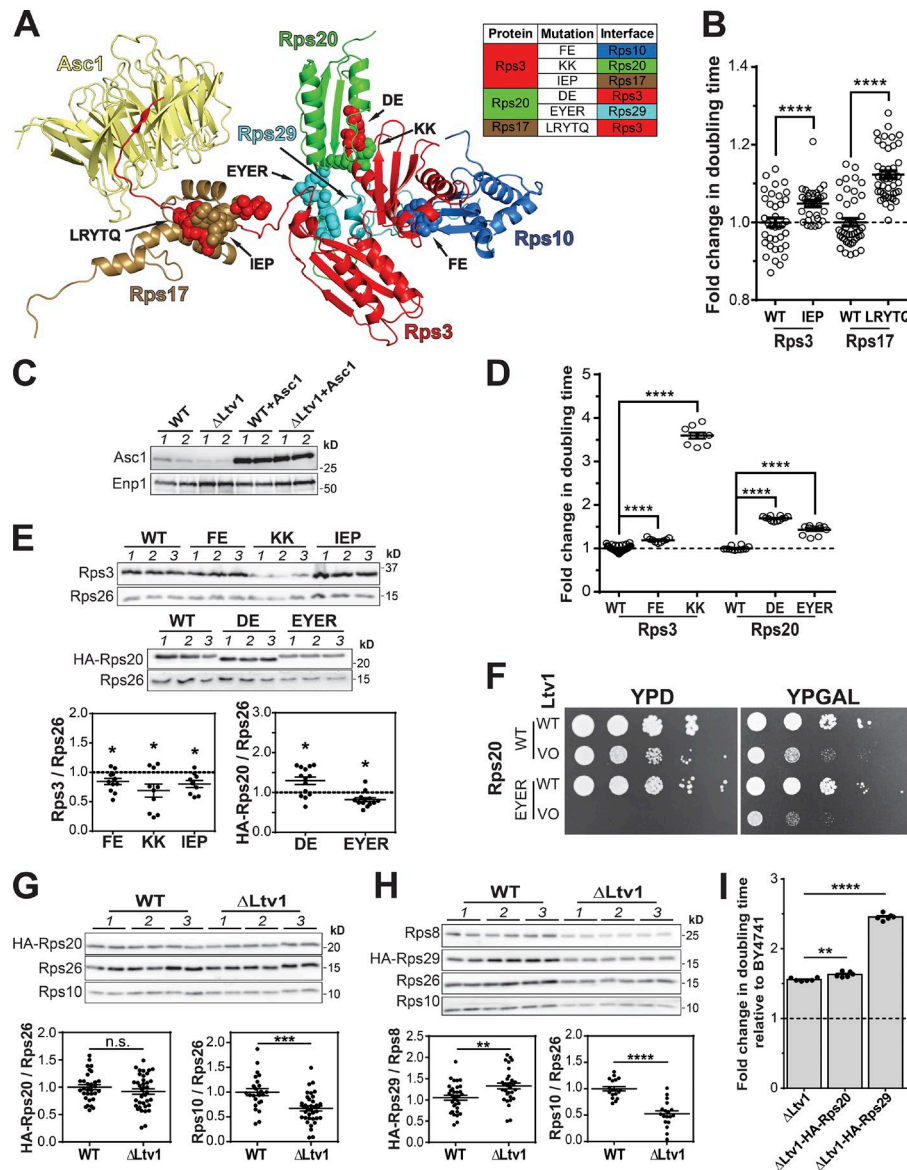


Figure S1. Growth defects of Rps3 network mutations. **(A)** Rps3 (red) interaction network with Rps10 (blue), Rps20 (green), Rps17 (brown), Rps29 (cyan), and Asc1 (yellow) on the beak structure of mature 40S ribosomes (PDB ID: 4V88). Table indicates the mutations between interacting proteins. **(B)** Growth defects from mutations at the Rps17/Rps3 interface in the presence of Ltv1 monitored by quantitative growth assays. $n = 9$ with five technical repeats. **(C)** Overexpression of Asc1 in cells containing a high copy number plasmid of Asc1. $n = 2$. **(D)** Growth defects from mutations in Rps3 and Rps20 in the presence of Ltv1. Fold-change values were determined by comparison of the effect from each mutation on growth relative to WT protein. $n = 3–4$ with three to four technical repeats. **(E)** Expression levels of Rps3 and HA-Rps20 mutants relative to Rps26 in the presence of Ltv1. $n = 3$ (labeled as 1, 2, and 3) with three to four technical repeats. **(F)** Serial dilutions demonstrate synthetic lethal interactions between Rps20_EYER and Ltv1 deletion. VO, vector only. **(G and H)** Changes in the occupancy of HA-Rps20 (G) and HA-Rps29 (H) were determined by Western blotting of ribosomes purified from WT and $\Delta Ltv1$ cells. $n = 3$ (labeled as 1, 2, and 3) with three technical repeats. **(I)** HA tagging Rps20 and Rps29 induces sensitivity to Ltv1 deletion. $n = 3$ with two technical repeats. The error bars represent the SEM, and significance was determined using an unpaired Student's *t* test. *, $P < 0.05$; **, $P < 0.01$; ***, $P < 0.001$; ****, $P < 0.0001$.

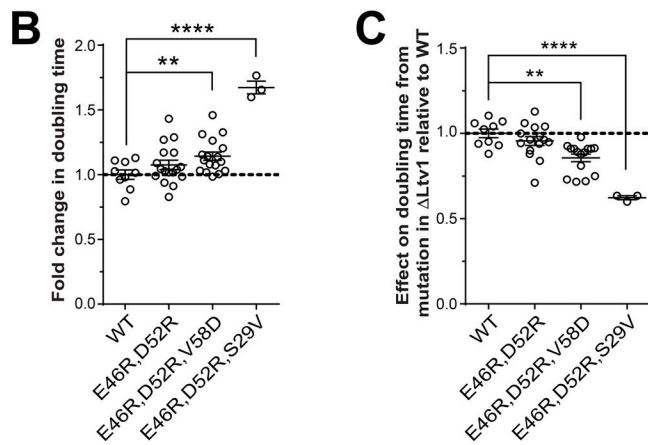
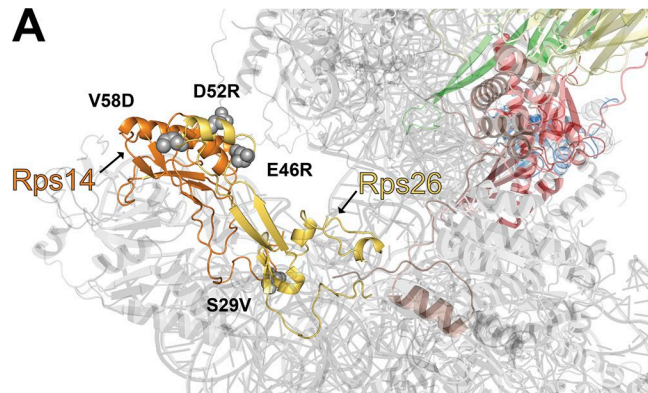


Figure S2. Effect of loss of Ltv1 on mutations in Rps26. **(A)** Structure of the platform region of the 40S subunit showing Rps26 (yellow) and mutations (gray) that disrupt interactions with Rps14 (orange) on the ribosome relative to the Rps3 network from Fig. S1 A. **(B)** Growth defects from mutations in Rps26 monitored by quantitative growth assays in cells containing Ltv1. **(C)** Rps26 mutants are resistant to Ltv1 deletion. Fold-change values were determined by comparison of the effects from Rps26 mutations in the presence or absence of Ltv1. The data are averages from three to five technical repeats of $n = 3$ biological replicates, the error bars represent the SEM, and significance was determined using an unpaired Student's *t* test. , **, $P < 0.01$; ****, $P < 0.0001$.

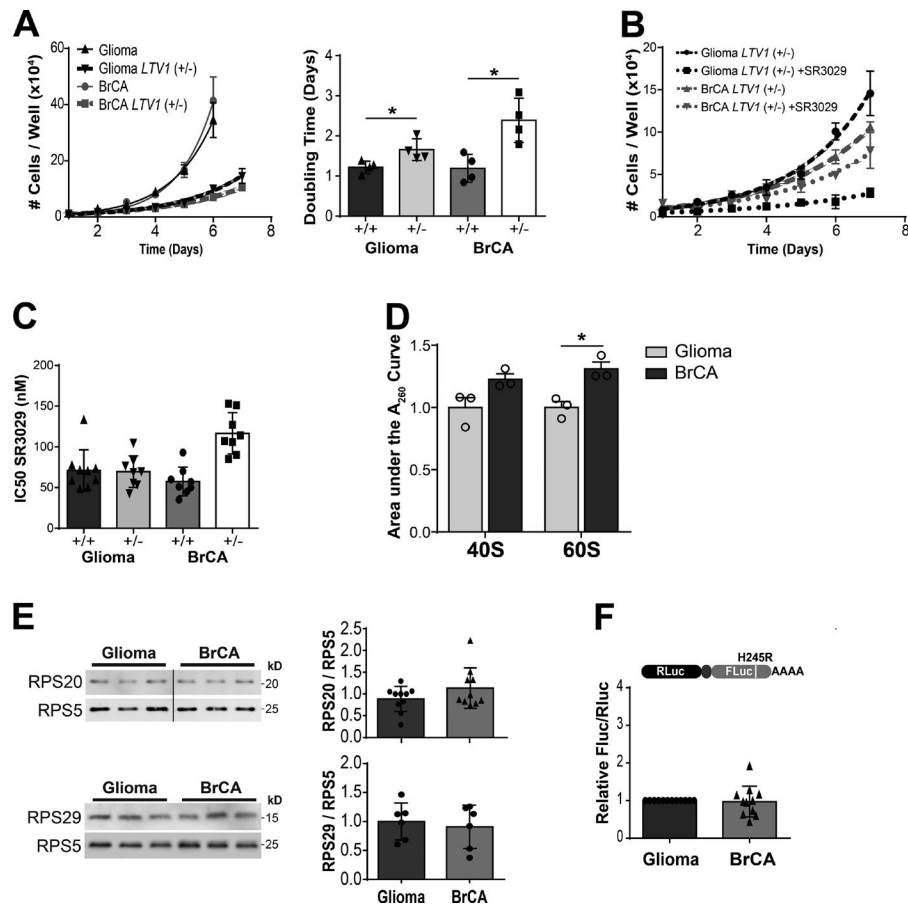


Figure S3. Glioma and breast cancer cells are differentially affected by Ltv1 deletion. **(A)** Effect of heterozygous knockouts of SF268 glioma and MDA-MB-231 breast cancer cells on growth ($n = 4$). **(B)** The effect on cellular growth from SR3029 treatment in SF268 glioma and MDA-MB-231 breast cancer cells ($n = 3$). **(C)** SR3029 sensitivity as measured by MTT assay ($n = 8-9$). **(D)** Quantification of 40S and 60S subunit levels from polysome profiles (area under the curve) of cell lysates supplemented with 15 mM EDTA to split 80S like ribosomes ($n = 3$). **(E)** Rps20 and Rps29 levels in ribosomes purified from glioma and breast cancer cells ($n = 6-10$). **(F)** Effects on decoding translational fidelity between glioma and breast cancer cells ($n = 12$). Error bars represent the SEM, and significance was determined using an unpaired Student's *t* test. *, $P < 0.05$.

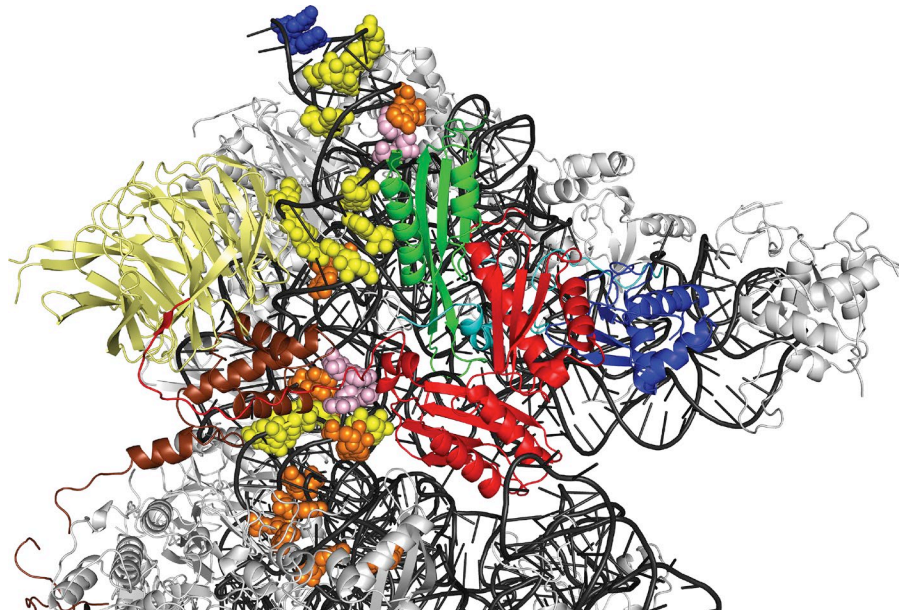


Figure S4. RimM and Ltv1 deletion produces similar changes in the small subunit head. rRNA residues that are protected by both Ltv1 and RimM are shown in pink spheres; residues made accessible by both Ltv1 and RimM are shown in blue spheres; residues protected only by Ltv1 are shown in orange; and residues protected only by RimM are shown in yellow. Note that Ltv1 probing accessed only A and C residues, whereas RimM probing accessed all residues.

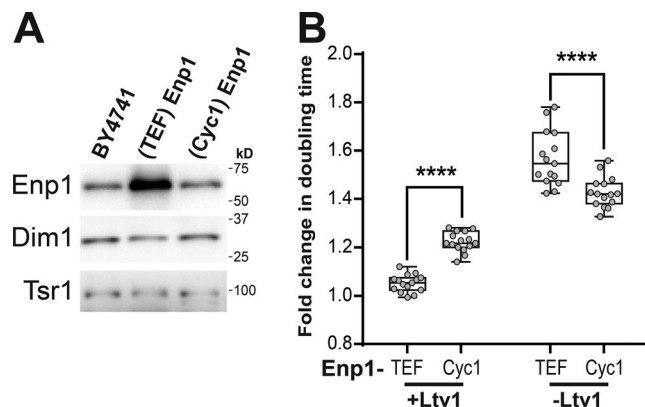


Figure S5. Effect of Enp1 expression on the loss of Ltv1. **(A)** Enp1 is overexpressed under the TEF promoter. **(B)** Growth defects from overexpression of Enp1 monitored by quantitative growth assays. The data are averages from five biological replicates with three technical replicates. The box represents the interquartile range with the line indicating the mean and the whiskers showing the min and maximum range. ****, P < 0.0001.

Table S1. Yeast strains used in this study

Strain	Description	Genotype	Reference
YKK493	Gal:Rps3	BY4741 (MAT α His3-1 Leu2-0 Met15-0 Ura3-0); Gal-Rps3::KAN	This work
YKK73	Δ Ltv1	BY4741; Ltv1::KAN	Open Biosystems
YKK762	Gal:Rps3; Δ Ltv1	BY4741; Gal-Rps3::NAT; Ltv1::KAN	This work
YKK729	Gal:Rps20; Δ Ltv1	BY4741; Gal-Rps20::HYG; Ltv1::KAN	This work
YKK730	Gal:Rps20	BY4741; Gal-Rps20::HYG	This work
YKK722	Tet:Rps10	BY4741; Rps10A::HYG; Rps10B::KAN w/pKK30034	Ferreira-Cerca et al. (2005)
YKK853	Gal:Rps29	BY4741; Gal-3HA-Rps29A::NAT; Rps29B::KAN	This work
YKK1115	Gal:Rps29; Δ Ltv1	BY4741; Gal-3HA-Rps29A::NAT; Rps29B::KAN; Ltv1::HYG	This work
YKK802	Gal:Rps17; Δ Ltv1	BY4741; Gal-Rps17B::NAT; Rps17A::KAN; Ltv1::HYG	This work
YKK427	Gal:Enp1	BY4741; Gal-Enp1::KAN	Ghalei et al. (2015)
YKK1142	Gal:Enp1; Δ Ltv1	BY4741; Gal-Enp1::KAN; Ltv1::HYG	This work
YKK479	Δ Asc1	BY4741; Asc1::KAN+ pKK3522	Thompson et al. (2016)
YKK479	Gal:Rps3; Δ Asc1	BY4741; Gal-Rps3::NAT; Asc1::KAN	This work
YKK1166	Gal:Rps26; Δ Ltv1	BY4741; Gal-Rps26A::NAT; Rps26B::KAN; Ltv1::HYG	This work

Table S2. Plasmids used in this study

Plasmid	Description	Reference
pKK3521	pRS416-TEF-Rps3	This work
pKK3525	pRS416-TEF-Rps3_(1-214)	This work
pKK3905	pRS416-TEF-Rps3_FE	This work
pKK3570	pRS416-TEF-Rps3_KK	This work
pKK3728	pRS416-TEF-Rps3_IRP	This work
pKK3786	pRS415-TEF-Rps10	This work
pKK3582	pRS413-TEF-Rps17	This work
pKK3775	pRS413-TEF-Rps17_LRYTQ	This work
pKK3890	pRS415-TEF-Rps20	This work
pKK3891	pRS415-TEF-Rps20_EYER	This work
pKK3934	pRS415-TEF-Rps20_DE	This work
pKK3944	pRS416-TEF-Rps29	This work
pKK30058	pRS416-TEF-3HA-Rps29	This work
pKK3606	pRS413-TEF-Ltv1	This work
pKK3842	pRS415-TEF-Ltv1	This work
pKK3541	pRS416-TEF-Enp1	This work
pKK30234	pRS415-Cyc1-Enp1	This work
pKK3547	pRS416-TEF-Asc1	This work
pKK3571	pRS415-GPD-Asc1	This work
pKK30251	pRS426-GPD-Asc1	This work
pKK30059	pRS415-ADH1/GPD-Start-site (Renilla(AUG)/Firefly(UUG))	Cheung et al. (2007)
pKK3923	pRS415-TEF-Read-through	Keeling et al. (2004)
pKK3924	pRS415-TEF-Stop	Keeling et al. (2004)
pKK3925	pRS415-TEF-Misincorporation (Firefly_H245R)	Salas-Marco and Bedwell (2005)
pKK3920	pRS415-ADH1-0 Frameshift Control	Harger and Dinman (2003)
pKK3921	pRS415-ADH1-liter _A (-1) Frameshift	Harger and Dinman (2003)
pKK3922	pRS415-ADH1-Ty1 (+1) Frameshift	Harger and Dinman (2003)
pKK3522	pRS413-U24	Li et al. (2009)
pKK523	pSpCas9n(BB)-2A-Puro (PX462) V2.0; Addgene plasmid 62987	Ran et al. (2013)
pKK524	pSpCas9n(BB)-2A-Puro (PX462)-Dir2	This work
pKK525	pSpCas9n(BB)-2A-Puro (PX462)-Ex2	This work
pKK518	pRM hRLuc-hFLuc H245R	Oishi et al. (2015)
pKK519	pRM hRLuc-hFLuc D357X	Oishi et al. (2015)
pKK30172	pSC40	Cole et al. (2009)
pKK30173	pSC40_A1492C	Cole et al. (2009)
pKK30034	pCM189-TET-Rps10	This work

Table S3. Oligonucleotides used in this study

DNA oligonucleotides	Sequence (5' to 3')	Name
hLT1 gRNA	CACCGAAGGATCTCGTTGGCTCCGG	Dir2
	AAACCCGGAGCCAACGAGATCCTT	Dir2C
	CACCGCAGATGAGACTGCACCCCCAG	Ex2
	AAACCTGGGTGCACTCTCATCTG	Ex2C
hLT1 exon2	GTGGCAGGCTTCTTGTCAATT	hLT1F
	CTGGCCAACGTGCTAACAGACT	hLT1R
hNB probes	TCTCCCTCCGAGTTCTCGCTCT	21S
	CCTGCCCTCCGGCTCCGTTAATGATC	18SE
	GCATGGCTTAATCTTGAGACAAGCATAT	18S
	AACGATCAGAGTAGTGGTATTCACC	28S
	ATCAGCACGGAGTTTGAC	SRP
	CGTGGAGTGGACGGAGCAAG	U2
Rps3_R64R65E	GATGTTTGGGTGAAAACGGTGAAGAAATCAACGAATTAACTTTGTTG	Rps3_RR
Rps3_E23E28R-F24A	GTCTTCTACGCTGAATTGAACAGAGCCTTCACCAGAACATTAGCTGAAGAAGGTTACTCC	Rps3_FE
Rps3_I207P211A-E210R	GCTTGGCCAGATGCTGTACCGCCATTGAGCAAAGAACAGAACCAATTCTTG	Rps3_IEP
Rps17_T39Q42A	GAGACTTTGTGATGAAATTGAGCTATCCGATCCAAGAGATTGAGAAACAAG	
Rps17_L16Y20A-R19E	GTCAAACGTGCCCTCCAAGGCTGCATTGAGAACAGCCTATCCAAGATTGACCTTGGATTTC	
Rps3-K7K10A	GTCGCTTAAATCTCTGCAAAAGAGCGCTAGTCGCTGACG	Rps3_KK
Rps20-E80E83K-Y82A-R85E	GGTTCTAACGACTTGGAAAACGCCAAATGAAATCCACAAGAGATAC	Rps20_EYER
Rps20-D113K_E155K	CCATTGAACCTGGTGTGAAGCTAACAGTTGTTGCTTC	Rps20_DE
Rps26-E46R	GAATGGCTATCAGAACATTGTTGAGCCGCTGCCGTAGAGATTGTC	Rps26_E46R
Rps26-D52R	CATTGTTGAAGCCGCTGCCGTAGACGTTGTCGAAGCTTGTCTACCCCTG	Rps26_D52R
Rps26-V58D	GTCAGAGATTGTCGAAGCTCTGACTACCCCTGAATACGCTTGCCAAAG	Rps26_V58D
Rps26-S29V	CCAGTCAGATGTCAACTTCAAGTTATTCAAAGATAAGGCTATCAAGAGAATG	Rps26_S29V
SHAPE-oligo-20S-1400	GCCTCAAACCTCCATCGGCTT	

References

- Cheung, Y.N., D. Maag, S.F. Mitchell, C.A. Fekete, M.A. Algire, J.E. Takacs, N. Shirokikh, T. Pestova, J.R. Lorsch, and A.G. Hinnebusch. 2007. Dissociation of eIF1 from the 40S ribosomal subunit is a key step in start codon selection in vivo. *Genes Dev.* 21:1217–1230. <https://doi.org/10.1101/gad.152830>
- Cole, S.E., F.J. LaRiviere, C.N. Merrikh, and M.J. Moore. 2009. A convergence of rRNA and mRNA quality control pathways revealed by mechanistic analysis of nonfunctional rRNA decay. *Mol. Cell.* 34:440–450. <https://doi.org/10.1016/j.molcel.2009.04.017>
- Ferreira-Cerca, S., G. Pöll, P.E. Gleizes, H. Tschochner, and P. Milkereit. 2005. Roles of eukaryotic ribosomal proteins in maturation and transport of pre-18S rRNA and ribosome function. *Mol. Cell.* 20:263–275. <https://doi.org/10.1016/j.molcel.2005.09.005>
- Ghalei, H., F.X. Schaub, J.R. Doherty, Y. Noguchi, W.R. Roush, J.L. Cleveland, M.E. Stroupe, and K. Karbstein. 2015. Hrr25/CK18-directed release of Ltv1 from pre-40S ribosomes is necessary for ribosome assembly and cell growth. *J. Cell Biol.* 208:745–759. <https://doi.org/10.1083/jcb.201409056>
- Harger, J.W., and J.D. Dinman. 2003. An in vivo dual-luciferase assay system for studying translational recoding in the yeast *Saccharomyces cerevisiae*. *RNA*. 9:1019–1024. <https://doi.org/10.1261/rna.5930803>
- Keeling, K.M., J. Lanier, M. Du, J. Salas-Marco, L. Gao, A. Kaenjak-Angeletti, and D.M. Bedwell. 2004. Leaky termination at premature stop codons antagonizes nonsense-mediated mRNA decay in *S. cerevisiae*. *RNA*. 10:691–703. <https://doi.org/10.1261/rna.5147804>
- Li, Z., I. Lee, E. Moradi, N.J. Hung, A.W. Johnson, and E.M. Marcotte. 2009. Rational extension of the ribosome biogenesis pathway using network-guided genetics. *PLoS Biol.* 7:e1000213. <https://doi.org/10.1371/journal.pbio.1000213>
- Oishi, N., S. Duscha, H. Boukari, M. Meyer, J. Xie, G. Wei, T. Schrepfer, B. Roschitzki, E.C. Boettger, and J. Schacht. 2015. XBP1 mitigates aminoglycoside-induced endoplasmic reticulum stress and neuronal cell death. *Cell Death Dis.* 6:e1763. <https://doi.org/10.1038/cddis.2015.108>
- Ran, F.A., P.D. Hsu, C.Y. Lin, J.S. Gootenberg, S. Konermann, A.E. Trevino, D.A. Scott, A. Inoue, S. Matoba, Y. Zhang, and F. Zhang. 2013. Double nicking by RNA-guided CRISPR Cas9 for enhanced genome editing specificity. *Cell*. 154:1380–1389. <https://doi.org/10.1016/j.cell.2013.08.021>
- Salas-Marco, J., and D.M. Bedwell. 2005. Discrimination between defects in elongation fidelity and termination efficiency provides mechanistic insights into translational readthrough. *J. Mol. Biol.* 348:801–815. <https://doi.org/10.1016/j.jmb.2005.03.025>
- Thompson, M.K., M.F. Rojas-Duran, P. Gangaramani, and W.V. Gilbert. 2016. The ribosomal protein Ascl/RACK1 is required for efficient translation of short mRNAs. *eLife*. 5:e11154. <https://doi.org/10.7554/eLife.11154>